Chapter 12
Evaluation of NVH in Lightweight Gears: An NL-ROM Study on Contact Ratio and Web Flexibility

Fabio Bruzzone, Carlo Rosso, and Daniele Fabbri

Abstract The drive for lightweight, power-dense, and quiet powertrains in EV and aerospace sectors demands predictive tools for complex gear dynamics. High Contact Ratio (HCR) gears (CR ¿ 2) and thin-webbed gear bodies are critical design strategies to improve NVH performance and reduce mass. However, these features introduce significant non-linearities and potential coupling between the gear mesh and structural dynamics, which are challenging to model accurately and efficiently. This study employs a validated, computationally efficient Non-linear Reduced Order Model (NL-ROM) to investigate these phenomena. The approach integrates the full flexibility of the gear bodies from a detailed Finite Element (FE) basis without geometric simplification, while also accounting for non-linear effects such as time-varying mesh stiffness, contact loss, and vibro-impacts. We extend the model's application to systematically analyze a series of spur gear pairs featuring different contact ratios (CR ¿ 2) and varying web thicknesses. The investigation focuses on the Dynamic Transmission Error (DTE) across a range of operating speeds and torques. A comparative analysis of the dynamic response is performed by post-processing the simulated DTE. This includes generating pseudo-experimental spectrograms to map the frequency content and amplitude of vibrations as a function of contact ratio and web flexibility. The results provide insights into the design trade-offs for modern gears, highlighting how specific geometric configurations can either mitigate or exacerbate vibrations. This work demonstrates the model's powerful capability as a high-fidelity predictive tool for the early-stage design and optimization of next-generation, lightweight gear systems.

Keywords gearbox · NVH · gears

Introduction

The automotive industry's shift towards electric powertrains, driven by environmental concerns, has introduced new challenges in Noise, Vibration, and Harshness (NVH). The absence of masking noise from internal combustion engines makes high-frequency gear whine, caused by gear meshing dynamics, a dominant and often undesirable acoustic feature. Consequently, mitigating gear noise at its source has become a critical focus for improving the perceived sound quality of electric vehicles. Similarly, the aviation industry's pursuit of higher power density and fuel efficiency has led to the adoption of lightweight gears, which can exhibit complex dynamic phenomena requiring detailed study to ensure safety and performance. The dynamic behavior of gear transmission systems has been extensively investigated through both theoretical and experimental methods [1, 2]. High-fidelity approaches, such as Finite Element (FE)/contact mechanics models, have provided deep insights. Parker and Vijayakar [3] introduced a model where dynamic mesh forces were calculated via detailed contact analysis at each time step, capturing non-linearities like contact loss but at a significant computational cost. This formulation was also applied to complex helicopter planetary gear systems [4]. Other research has focused on the influence of tooth surface modifications on Static and Dynamic Transmission Error (STE, DTE) through analytical solutions [5] and comprehensive experiments [6]. A significant body of work has explored the rich non-linear dynamics arising from gear backlash, time-dependent mesh stiffness, and bearing clearances. These studies have identified complex behaviors including periodic, quasi-periodic, and chaotic motions using both analytical and numerical methods [7, 8, 9, 10], and have investigated

Fabio Bruzzone · Carlo Rosso · Daniele Fabbri
Department of Mechanical and Aerospace Engineering
Politecnico di Torino, TO 10129, Italy
e-mail: fabio.bruzzone@polito.it; carlo.rosso@polito.it; daniele.fabbri@polito.it

Kristin B. Zimmerman, PhD (eds.), *Nonlinear Structures & Systems, Vol. 1*, Conference Proceedings of the Society for Experimental Mechanics Series, https://doi.org/10.1007/978-8-743-81440-5_12

resonances in planetary systems [11]. However, many of these works either require substantial computational resources or employ simplified gear geometries, limiting their direct application in all design scenarios. To bridge the gap between accuracy and efficiency, various hybrid and reduced-order methods have been developed. For instance, hybrid FE-Analytical approaches have been used to analyze transmission error in lightweight gears [12], and multibody models have incorporated precomputed look-up tables for contact conditions [13]. Other hybrid methods combine FE static analysis with analytical vibration models to reduce computation time [14]. While effective, these methods often introduce compromises, such as assuming rigid gear bodies [13], neglecting gear blank flexibility [14], or simplifying geometry by removing teeth [15], which can limit their applicability, especially for thin-walled gears where body flexibility is crucial.

This paper presents a novel model designed to overcome these limitations. We detail a Non-linear Reduced Order Model (NL-ROM) that simulates the true rolling motion and engagement of a gear pair. To our knowledge, simulating the actual rotation and moving contact point using a ROM has not been previously reported. The model inherently captures the non-linearity of the moving contact point, amplified by a load-dependent Time-Varying Mesh Stiffness (TVMS). Contact loss is explicitly handled, and reconnection is treated as a Vibro-Impact (VI). A key advantage is that the full flexibility of axisymmetric gear bodies is retained from the underlying FE model without geometric simplification, even with a minimal set of master Degrees of Freedom (DoFs). This drastically reduces matrix sizes, enabling long time-domain simulations with minimal computational cost and high accuracy. The model's predictions are validated against a high-quality experimental campaign on a gear pair exhibiting complex non-linear phenomena, showing remarkable agreement with DTE measurements.

Methodology

This section details the iterative algorithm for obtaining the time-domain response of a gear pair. The method employs a pre-processing phase to generate a ROM that significantly reduces computational cost. The periodic nature of gear meshing is exploited by leveraging the cyclic symmetry of the gear geometry. The properties of the FE model are considered periodic over an angle $\theta = 360/Z_p$, where Z_p is the number of pinion teeth.

To simulate rotation, a set of reduced mass and stiffness matrices is pre-computed for N discrete angular positions within one mesh cycle. At each z^{th} angular position ($z = 1, ..., N$), the full FE mass and stiffness matrices ($\boldsymbol{K_{p,z}}$, $\boldsymbol{M_{p,z}}$, $\boldsymbol{K_{g,z}}$, $\boldsymbol{M_{g,z}}$) for the pinion (p) and gear (g) are reduced using the Craig-Bampton Component Mode Synthesis (CB-CMS) method [16]. The reduced system matrices at position z are given by:

$$\boldsymbol{M_z^r} = \begin{bmatrix} \boldsymbol{T_{p,z}^T} & \boldsymbol{T_{g,z}^T} \end{bmatrix} \begin{bmatrix} \boldsymbol{M_{p,z}} & \boldsymbol{0} \\ \boldsymbol{0} & \boldsymbol{M_{g,z}} \end{bmatrix} \begin{bmatrix} \boldsymbol{T_{p,z}} \\ \boldsymbol{T_{g,z}} \end{bmatrix} \tag{1}$$

and similarly for the system stiffness matrix $\boldsymbol{K_z^r}$, where $\boldsymbol{T_{p,z}}$ and $\boldsymbol{T_{g,z}}$ are the CB-CMS transformation matrices. The reduction basis consists of master nodes for force exchange and auxiliary observed nodes to improve the ROM's accuracy. As shown in Figure 1, these nodes are categorized as:

- **Contact mesh stiffness nodes** ($\boldsymbol{u_{Kc,p}}$, $\boldsymbol{u_{Kc,g}}$): These nodes, located on the tooth flanks, are where the time-varying contact stiffness is applied, serving as the primary source of excitation and non-linearity.
- **Auxiliary observed nodes** ($\boldsymbol{u_{aux,p}}$, $\boldsymbol{u_{aux,g}}$): Selected using a Modal-Geometrical Selection Criterion (MoGeSeC) [17], these nodes capture the highest modal content to enhance the ROM's accuracy for the frequency range of interest.
- **Central virtual nodes** ($\boldsymbol{u_{t,p}}$, $\boldsymbol{u_{t,g}}$): These master nodes are linked to the inner radii via rigid joints. All their DoFs are constrained except for rotation about the gear axis, where torque is applied. This setup mimics the experimental test bench, isolating the gear mesh dynamics.

The DTE is calculated from the angular displacement of these central nodes as:

$$DTE(t) = \theta_p(t) r_{b,p} - \theta_g(t) r_{b,g} \tag{2}$$

where $r_{b,p}$ and $r_{b,g}$ are the respective base radii. The accuracy of the ROM was validated through extensive modal analysis, showing excellent agreement with the full FE model (e.g., maximum frequency error of -0.05% and minimum MAC value of 88.9% for the pinion's first ten flexible modes).

The coupling between the pinion and gear is modeled by a time-varying, load-dependent contact stiffness matrix $\boldsymbol{K_c}(z, L)$, which connects the corresponding contact nodes. The TVMS value $k_c(z, L)$ is derived from pre-computed Static Transmission Error curves [18, 19, 20].

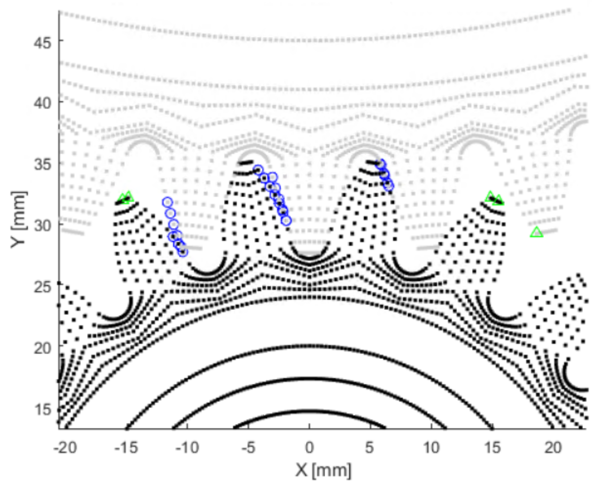

Fig. 1 Detail of the gear pair FE mesh and contact mesh stiffness nodes and auxiliary virtual nodes highlighted

The dynamic response is obtained using a Newmark direct time integration scheme [21] with parameters $\alpha_{NM} = 1/4$ and $\delta_{NM} = 1/2$ for unconditional stability without numerical damping. The system of equations to be solved at each timestep i (corresponding to angular position z) is:

$$\ddot{\boldsymbol{u}}_{\boldsymbol{i}} = \boldsymbol{S}_{\boldsymbol{i}}^{-1}\boldsymbol{\delta r_i} \tag{3}$$

where $\boldsymbol{S_i} = \boldsymbol{M}^r_{\boldsymbol{z},\boldsymbol{i}} + \Delta t_i \boldsymbol{C}^r_{\boldsymbol{z},\boldsymbol{i}} + \Delta t_i^2 \alpha_{NM}(\boldsymbol{K}^r_{\boldsymbol{z},\boldsymbol{i}} + \boldsymbol{K}^r_{\boldsymbol{c}}(z, L))$ and $\boldsymbol{\delta r_i}$ is the residual vector. The time step Δt_i varies with rotational speed to ensure that each step corresponds to a fixed angular increment $\Delta\theta_p$.

To simulate continuous rotation, the displacement, velocity, and acceleration vectors $(\boldsymbol{u}^*_{\boldsymbol{i}}, \dot{\boldsymbol{u}}^*_{\boldsymbol{i}}, \ddot{\boldsymbol{u}}^*_{\boldsymbol{i}})$ computed at step i are transformed using a rotation matrix $\boldsymbol{R_{\Delta\theta}}$ to serve as initial conditions for step $i + 1$, which uses the matrices for position $z + 1$.

$$\boldsymbol{u_i} = \boldsymbol{R_{\Delta\theta}}\boldsymbol{u}^*_{\boldsymbol{i}}, \quad \dot{\boldsymbol{u}}_{\boldsymbol{i}} = \boldsymbol{R_{\Delta\theta}}\dot{\boldsymbol{u}}^*_{\boldsymbol{i}}, \quad \ddot{\boldsymbol{u}}_{\boldsymbol{i}} = \boldsymbol{R_{\Delta\theta}}\ddot{\boldsymbol{u}}^*_{\boldsymbol{i}} \tag{4}$$

At the end of a mesh cycle ($z = N$), a special procedure ensures continuity. The ROM results are expanded to the full FE model, the nodes are re-sorted to advance the gear by one tooth, and the system state is reduced back to the initial ROM basis ($z = 1$) to begin the next cycle.

Further non-linearity is introduced by modeling contact loss. At each timestep, the normal force on each contact spring is checked. If a traction force is detected, that spring's contribution is set to zero, and the timestep is re-calculated iteratively until only compressive or null forces remain. This process is outlined in Figure 2. When a disconnected contact re-engages, the event is treated as a VI [22]. A discontinuity in velocities is imposed based on a coefficient of restitution e, while displacements remain continuous:

$$\begin{aligned} \dot{\boldsymbol{u}}^+_{\boldsymbol{Kc,g,n}} &= \frac{\dot{\boldsymbol{u}}^-_{\boldsymbol{Kc,g,n}}(1 - \epsilon \cdot e) + \epsilon \dot{\boldsymbol{u}}^-_{\boldsymbol{Kc,p,n}}(e + 1)}{1 + \epsilon} \\ \dot{\boldsymbol{u}}^+_{\boldsymbol{Kc,p,n}} &= \frac{\dot{\boldsymbol{u}}^-_{\boldsymbol{Kc,g,n}}(1 + e) + \epsilon \dot{\boldsymbol{u}}^-_{\boldsymbol{Kc,p,n}}(\epsilon - e)}{1 + \epsilon} \end{aligned} \tag{5}$$

where ϵ is the ratio of the equivalent masses of the impacting bodies. This comprehensive approach allows the model to capture a wide range of non-linear dynamic phenomena with high accuracy and computational efficiency. Further details and a comprehensive validation of the model presented are available in [23].

Case Study and Results

This section presents and analyzes the dynamic response of the High Contact Ratio (HCR) spur gear pair detailed in Table 1, with the notable design modification of having dissimilar web thicknesses for the pinion (12 mm) and gear (4 mm) as

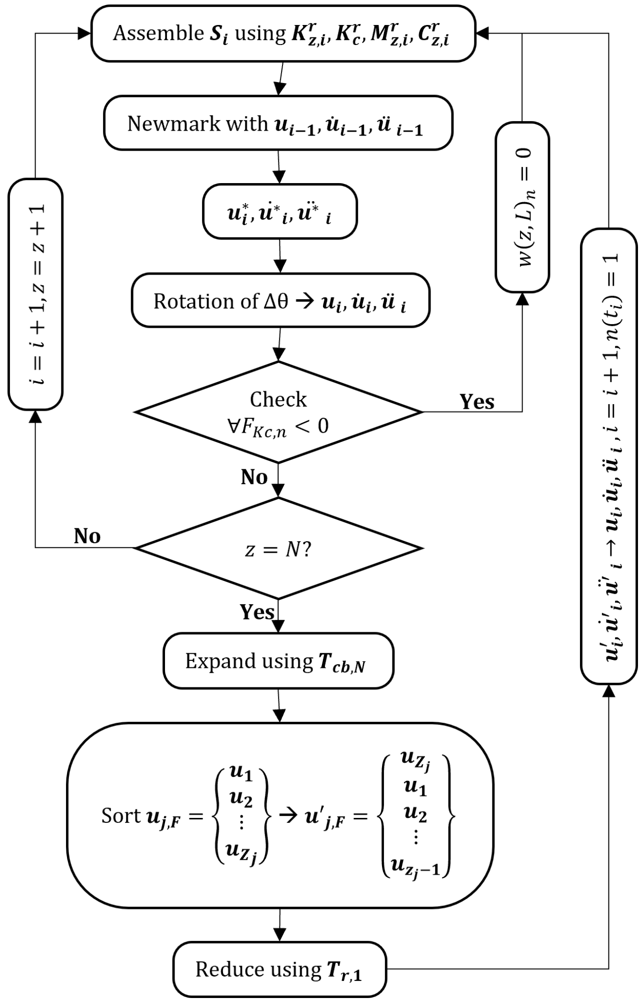

Fig. 2 Algorithm of the NL ROM

Table 1 Pinion and gear geometrical and material data

Parameter	Value	Unit
Pinion number of teeth, Z_1	21	-
Gear number of teeth, Z_2	71	-
Module, m	3	mm
Module, m	3	mm
Dedendum, h_f	1.45	-
Addendum, h_a	1.3	-
Facewidth, F	20	mm
Pinion base radius, r_b	29.6	mm
Gear base radius, r_b	100.07	mm
Total backlash, $2B$	0.125	mm
Contact ratio	2.12	-
Modulus of elasticity, E	207	GPa
Density, ρ	7600	kg/m^3
Poisson ratio, ν	0.3	-
Coefficient of restitution, e	0.56	-
Full FE number of DoFs	536004	-
Coupled ROM number of DoFs	484	-

well as having non-standard addendum and dedendum factors. The system's behavior was investigated under three distinct torque levels, namely 15 Nm, 50 Nm, and 100 Nm across a speed-up maneuver from 1000 to 5000 rpm over a 20 second duration. The results, obtained using the computationally efficient NL-ROM, are presented as pairs of plots: a spectrogram illustrating the harmonic content of the Dynamic Transmission Error (DTE) versus rotational velocity, and a corresponding plot of the mean DTE amplitude, obtained as the difference between the mean value of the STE and the mean value of the DTE in the time domain, averaged across one full revolution of the gear. The 4-hour simulation time for each extensive sweep highlights the model's capability for practical design exploration. The analysis reveals a highly non-linear system whose dynamic character changes profoundly with operating torque, demonstrating complex phenomena and load-dependent response stabilization although no contact loss event or VI has been detected in any simulation. A visualization of the FE connections of the contact nodes employed in the model is visible in Figure 5 for a single position and load. A visualization of the harmonic content of the TVMS for the current case study is visibile in Figure 3. A powerful implication of the proposed methodology is to visualize and appreciate the influence of coupled flexible modes of the system. In the current configuration a coupled mode as visible in Figure 4 is present at a meshing frequency close to 3000 rpm which will be important in the results to follow.

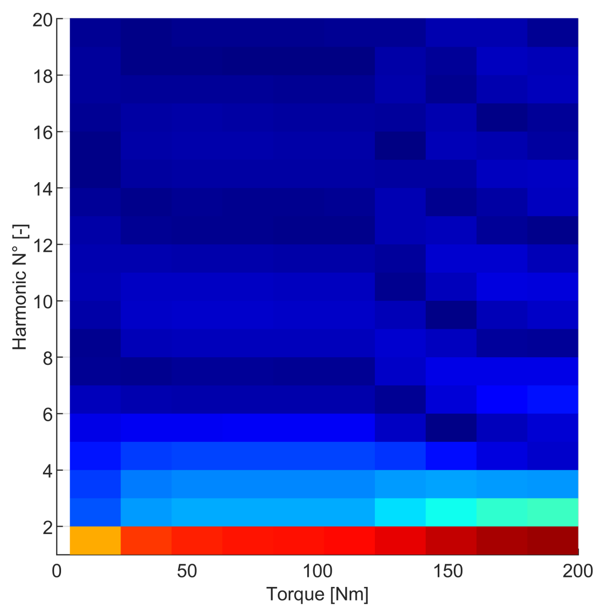

Fig. 3 Harmonic content of the TVMS for the HCR gear pair

At the lowest torque level of 15 Nm (Figure 6), the gear pair exhibits a dramatic and highly localized dynamic response. The mean DTE plot is dominated by an exceptionally sharp and high-amplitude resonance peak, reaching approximately 105 μm at a rotational velocity of about 2750 rpm. The narrowness of this peak suggests a lightly damped system mode is being strongly excited. Outside of this critical speed region, the system is relatively quiet, with only minor DTE fluctuations observed at lower speeds (e.g., around 1300 rpm). Observing the corresponding spectrogram at the 2750 rpm peak, the vibrational energy is not concentrated at the fundamental gear mesh frequency (Harmonic N° 1). Instead, the second, third, and fourth harmonics show significantly higher energy content, as indicated by the red and yellow coloring. This signifies a strong non-linear interaction, where energy from the primary mesh excitation is being channeled into higher-frequency super-harmonics. Above 3000 rpm, the system becomes remarkably stable, with negligible DTE across all harmonics. Increasing the torque to 50 Nm fundamentally alters the system's dynamic behavior as visible in Figure 7, leading to a counterintuitive reduction in overall vibration amplitude. The single, sharp resonance peak observed at 15 Nm is completely suppressed. In its place, the mean DTE plot shows a much broader and lower-amplitude response distributed across a wide speed range from approximately 1200 to 3200 rpm. The maximum DTE is now only about 36 μm, occurring near 2900 rpm, which is a nearly three-fold reduction compared to the low-torque case. Multiple smaller peaks are now evident, indicating that several system modes may be lightly excited, but none dominate the response in the same way. The spectrogram for the 50 Nm case is visibly "busier," confirming a change in the underlying dynamics. Vibrational energy is now spread across a wider array of harmonics, extending up to the 12th harmonic and beyond in the 2000-3000 rpm range. This suggests that

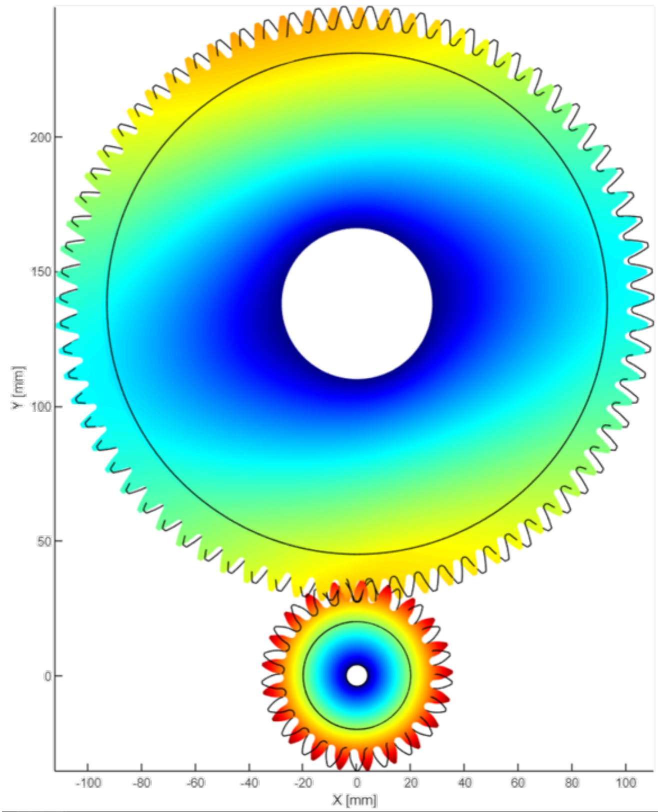

Fig. 4 Coupled modal response at 1050 Hz

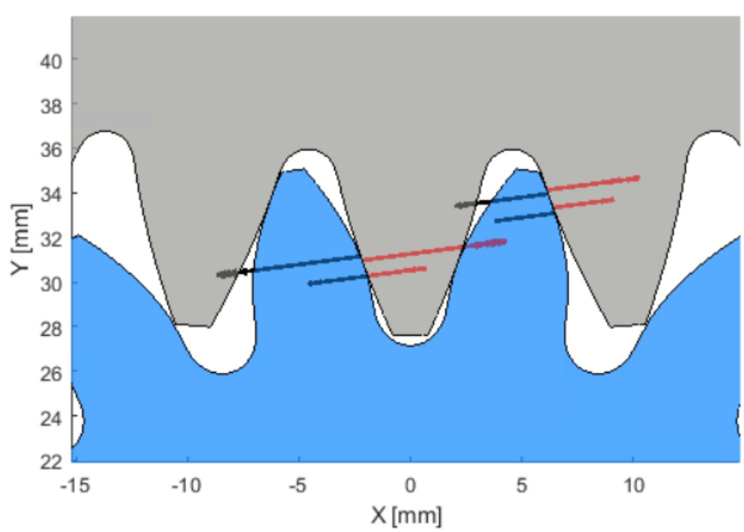

Fig. 5 Visualization of the contact nodes and stiffnesses in the FEM

while the severe, singular resonance is avoided, the system experiences more frequent, lower-intensity events, resulting in a richer, broadband harmonic spectrum. At the highest simulated torque of 100 Nm depicted in Figure 8, the system's response evolves once again, presenting a hybrid of the behaviors seen at the lower loads. The mean DTE plot shows the re-emergence of distinct resonant peaks. A dominant peak appears around 2950 rpm, reaching an amplitude of approximately 72 µm. While significant, this is still considerably lower than the 105 µm peak at 15 Nm. A secondary, but also prominent, peak is visible at a lower speed of around 1300 rpm, with an amplitude of about 40 µm. The spectrogram reveals that, similar to the 15 Nm

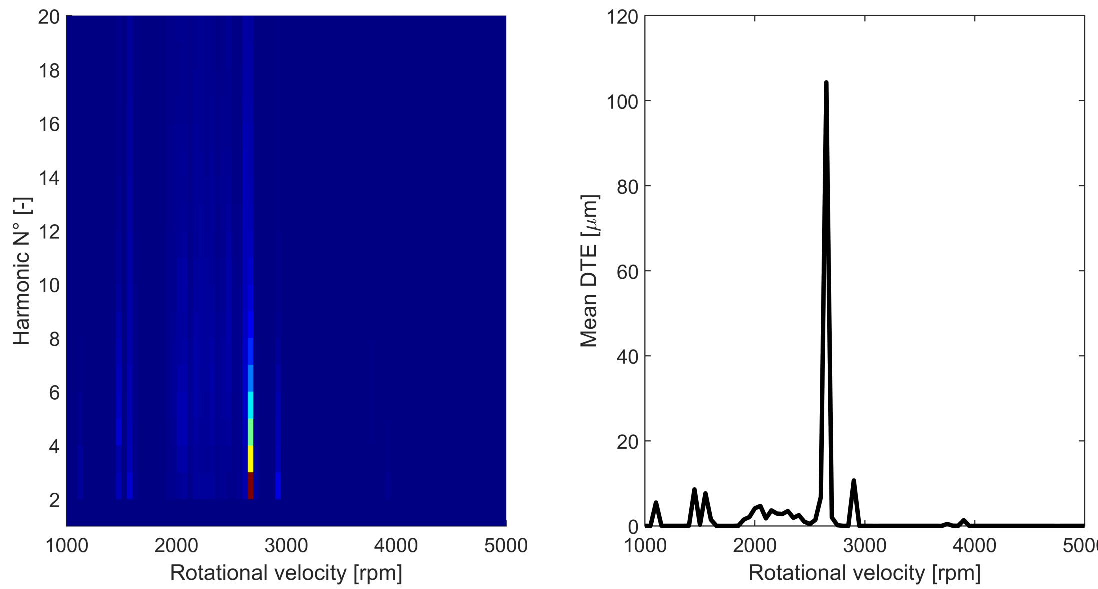

Fig. 6 Results at 15Nm

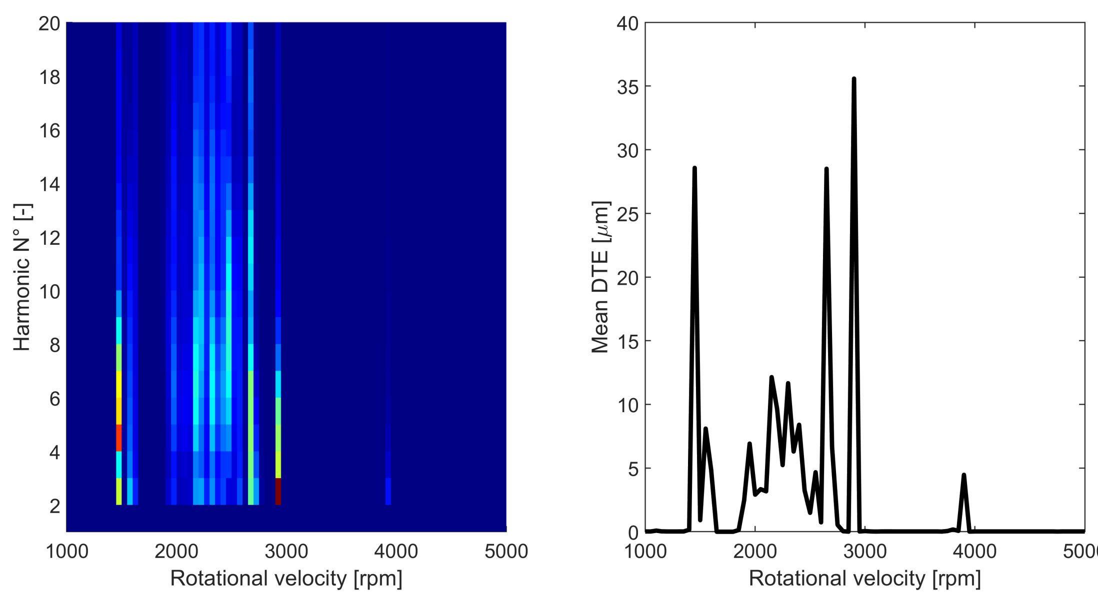

Fig. 7 Results at 50Nm

case, the energy at the main resonance near 2950 rpm is concentrated in the second and third harmonics, reaffirming the non-linear transfer of energy to super-harmonics. However, unlike the 15 Nm case, there is also a broader distribution of energy across other harmonics and speeds, reminiscent of the 50 Nm behavior. This suggests that at 100 Nm the magnitude of the TVMS, primary excitation source, is now significantly larger due to the higher transmitted load. This stronger excitation is sufficient to re-excite system resonances, though with a different character and amplitude compared to the resonance at low torque. The significant response at 1300 rpm may correspond to the excitation of a different system mode or a sub-harmonic resonance that becomes prominent only at higher load levels.

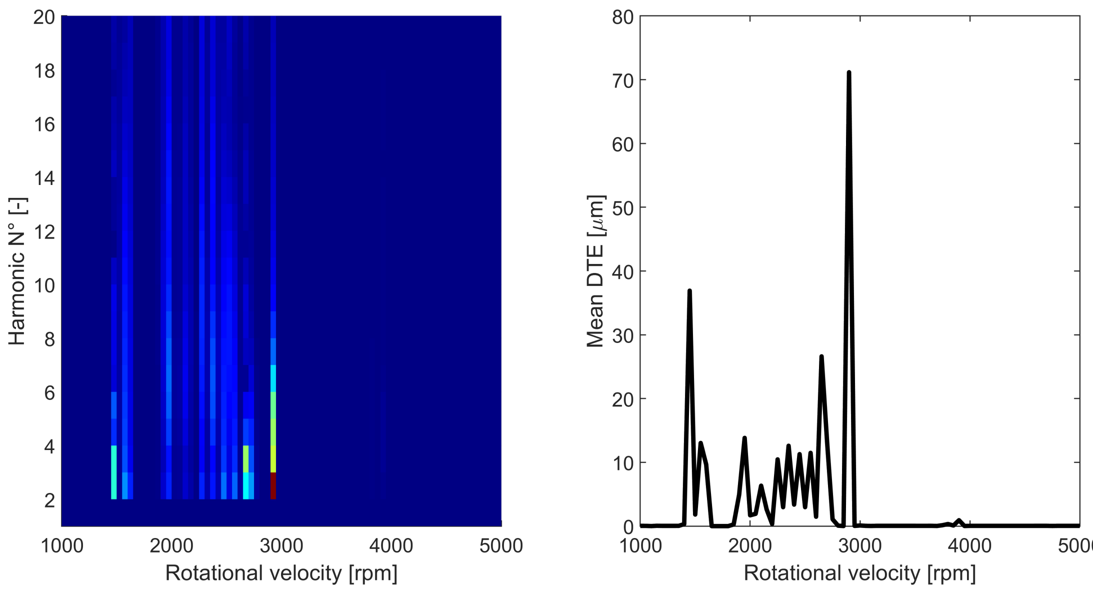

Fig. 8 Results at 100Nm

Conclusions

In this study, a computationally efficient NL-ROM was presented and employed to investigate the complex dynamic behavior of modern lightweight gear systems. The proposed methodology successfully bridges the gap between high-fidelity simulation and computational feasibility by retaining the full geometric detail of the flexible gear bodies from an underlying FE model while drastically reducing the system's degrees of freedom. A key innovation is the simulation of the gear's rolling motion by stepping through a pre-computed set of reduced matrices, which accurately captures the time-varying nature of the system. The model's predictive power is further enhanced by its ability to account for critical non-linear phenomena, including load-dependent TVMS, partial or total contact loss, and the subsequent VI upon tooth reconnection. The model was applied to analyze the dynamic response of a HCR spur gear pair with dissimilar web thicknesses under various operating conditions. The results revealed a profound and highly non-linear dependence of the DTE on the applied torque, showing that, for this scenario, at low torque the dynamic response is high, while a stabilizing effect is visible in the middle range. When the torque was increased further, resonant behavior re-emerged, though with a different character and lower peak amplitude than the low-torque case. These findings underscore the critical importance of analyzing gear dynamics across a full range of operating conditions, as system behavior at a single load point is not indicative of the overall performance. The demonstrated capability of the NL-ROM validates it as a powerful and practical tool for virtual prototyping and optimization in the early design stages of next-generation powertrains, enabling engineers to identify and mitigate potential NVH issues and explore complex design trade-offs with confidence and efficiency.

Acknowledgments This publication is part of the project PNRR-NGEU which has received funding from the MUR – DM 117/2023

References

1. Ozguven, H.N. and Houser, D.R. "Mathematical models used in gear dynamics - a review". *Journal of Sound and Vibration*, 121(3):383–411 (1988).
2. Bruzzone, F. and Rosso, C. "Sources of excitation and models for cylindrical gear dynamics: A review". *Machines*, 8(3) (2020).
3. Parker, R.G., Vijayakar, S.M., and Imajo, T. "Non-linear dynamic response of a spur gear pair: Modelling and experimental comparisons". *Journal of Sound and Vibration*, 237(3):435–455 (2000).
4. Parker, R.G., Agashe, V., and Vijayakar, S.M. "Dynamic response of a planetary gear system using a finite element/contact mechanics model". *Journal of Mechanical Design*, 122:304–310 (2000).
5. Eritnel, T. and Parker, R.G. "Nonlinear vibration of gears with tooth surface modifications". *Journal of Vibration and Acoustics*, 135:(051005)1–11 (2013).

6. Benatar, M., Handschuh, M., Kahraman, A., and Talbot, D. "Static and dynamic transmission error measurements of helical gear pairs with various tooth modifications". *Journal of Mechanical Design*, 141:103301 (2019).
7. Theodossiades, S. and Natsiavas, S. "Non-linear dynamics of gear-pair systems with periodic stiffness and backlash". *Journal of Sound and Vibration*, 229(2):287–310 (2000).
8. Natsiavas, S. and Giagopoulos, D. "25 - non-linear dynamics of gear meshing and vibro-impact phenomenon". pages 773–792 (2010).
9. Natsiavas, S. "Analytical Modeling of Discrete Mechanical Systems Involving Contact, Impact, and Friction". *Applied Mechanics Reviews*, 71(5):050802 (2019).
10. Wang, X.S., Wu, S.J., Hu, J.C., and Chen, J. "Chaos and bifurcation analysis of gear pair with wear fault". In *Material Sciences and Manufacturing Technology*, volume 629 of *Advanced Materials Research*, pages 506–510. Trans Tech Publications Ltd (2013).
11. Mohammadpour, M., Theodossiades, S., and Rahnejat, H. "Dynamics and efficiency of planetary gear sets for hybrid powertrains". *Proceedings of the Institution of Mechanical Engineers, Part C: Journal of Mechanical Engineering Science*, 230(7-8):1359–1368 (2016).
12. Shweiki, S., Rezayat, A., Tamarozzi, T., and Mundo, D. "Transmission error and strain analysis of lightweight gears by using a hybrid fe-analytical gear contact model". *Mechanical Systems and Signal Processing*, 123:573–590 (2019).
13. Palermo, A., Mundo, D., Hadjit, R., and Desmet, W. "Multibody element for spur and helical transmission error and the dynamic stress factor of spur gear pairs.". *Mechanism and Machine Theory*, 62:13–30 (2013).
14. Dai, X., Cooley, C.G., and Parker, R.G. "An efficient hybrid analytical-computational method for nonlinear vibration of spur gear pairs". *Journal of Vibration and Acoustics*, 141:(011006)1–13 (2018).
15. Guilbert, B., Velex, P., and Cutuli, P. "Quasi-static and dynamic analyses of thin-webbed high-speed gears: Centrifugal effect influence". *Proceedings of the Institution of Mechanical Engineers, Part C: Journal of Mechanical Engineering Science*, 233(21-22):7282–7291 (2019).
16. Craig, R.R. and Bampton, M.C.C. "Coupling of substructures for dynamic analyses". *AIAA Journal*, 6:1313–1319 (1968).
17. Bonisoli, E., Delprete, C., and Rosso, C. "Proposal of a modal-geometrical-based master nodes selection criterion in modal analysis". *Mechanical Systems and Signal Processing*, 23:606–620 (2009).
18. Rosso, C., Bruzzone, F., Maggi, T., and Marcellini, C. "A proposal for semi-analytical model of teeth contact with application to gear dynamics". *2019 JSAE/SAE Powertrains, Fuels and Lubricants* (2019).
19. Bruzzone, F., Maggi, T., Marcellini, C., and Rosso, C. "2d nonlinear and non-hertzian gear teeth deflection model for static transmission error calculation". *Mechanism and Machine Theory*, 166 (2021).
20. Bruzzone, F., Maggi, T., Marcellini, C., and Rosso, C. "Gear teeth deflection model for spur gears: Proposal of a 3d nonlinear and non-hertzian approach". *Machines*, 9(10) (2021).
21. Newmark, N.M. "A method of computation for structural dynamics". *Journal of the Engineering Mechanics Division*, 85:67–94 (1959).
22. Karayannis, I., Vakakis, A.F., and Georgiades, F. "Vibro-impact attachments as shock absorbers". *Proceedings of the Institution of Mechanical Engineers, Part C: Journal of Mechanical Engineering Science*, 222(10):1899–1908 (2008).
23. Bruzzone, F., Rosso, C., and Theodossiades, S. "Dynamic reduction technique for nonlinear analysis of spur gear pairs". *Nonlinear Dynamics*, 112:15797–15811 (2024).